JOURNAL OF MATERIALS SCIENCE **37** (2002) 4819–4829

Templating porosity in polymethylsilsesquioxane coatings using trimethylsilylated hyperbranched polymers

C. J. G. PLUMMER*, L. GARAMSZEGI*, T.-Q. NGUYEN†, M. RODLERT*, J.-A. E. MÅNSON*,†,‡

*Laboratoire de Technologie des Composites et Polymères (LTC) and †Laboratoire de Polymères (LP), Ecole Polytechnique Fédérale de Lausanne (EPFL), CH-1015, Switzerland
E-mail: jan-anders.manson@epfl.ch

A series of trimethylsilyl end-functionalized aliphatic hyperbranched polymers has been used to template porosity in polymethylsilsesquioxane films prepared by heat treatment of a spin cast methylsilsesquioxane precursor. By varying the extent of the end-functionalization, closed pore foams with controlled pore sizes and pore contents of up to 40 vol% were obtained by chemically-induced phase separation and thermal degradation of the hyperbranched polymers during the heat treatment.

1. Introduction

Thermal degradation of polymer templates to induce porosity in heat resistant organic or inorganic films has principally been developed in response to the need for low dielectric constant, ε, heat resistant insulating materials in the electronics industry [1]. At present levels of integration (device sizes below 1 μm), signal delays are dominated by the capacitative resistance of the interconnect array and there is consequently an approximately linear relationship between signal delay times and ε [2]. Any reduction in this latter will therefore have immediate benefits for performance. Silicate glass (SiO_2), the conventional insulating material, has a relatively high ε of between 4 and 4.2, whereas the demand is now for materials with ε in the range 2 to 2.5, and projected levels of integration are likely to require $\varepsilon < 2$. However, replacement of SiO_2 by many types of low ε-material, typified by aliphatic fluorinated polymers, remains unfeasible owing to the high thermal stability required for metallization, which imposes temperatures of at least 400°C and processing times of at least 1 h [1]. Such materials may also fail to meet other requirements including low moisture absorption, good adhesion to metals and inorganic oxides, and high mechanical toughness and hardness. In porous media, ε decreases roughly linearly with pore content [3], approaching $\varepsilon \approx 1$ as the porosity tends to 100 vol%. This not only permits reduction of ε without altering other materials characteristics, but, given that the lowest known bulk value for ε is 2 (polytetrafluoroethylene), it is also at present the only way of obtaining solid insulating materials with $\varepsilon < 2$. Additional criteria imposed on porous materials by integrated circuit technology are closed-cell porosity and pore diameters well below the minimum lateral dimensions of the circuit elements, which are likely to decrease to close to 100 nm in the near future. There has consequently been substantial effort to develop aero- and xerogels by sol-gel reactions of orthosilicate esters [4] and mesoporous SiO_2 by self-organization in silica-surfactant systems [5]. However, these require complex, time intensive processing, and are limited by their intrinsically high matrix dielectric constant, so that relatively high levels of porosity are needed to reach a given target value of ε.

Another way of introducing nanoporosity into a thermally stable matrix is to modify it with a template consisting of a thermally labile species with the appropriate morphology [6–13]. The template is decomposed and removed by heat treatment, ideally leaving commensurate pores. A wide variety of molecular architectures have been synthesized for this purpose, ranging from polyimide precursors with thermally labile side chains [11, 13], to dendritic and multiarm star-shaped polymers for templating porosity in inorganic–organic hybrid polymethylsilsesquioxane (PMSSQ) films derived from methylsilsesquioxane (MSSQ) precursors [12] (Scheme I). If nanoporous foams with closed-cell

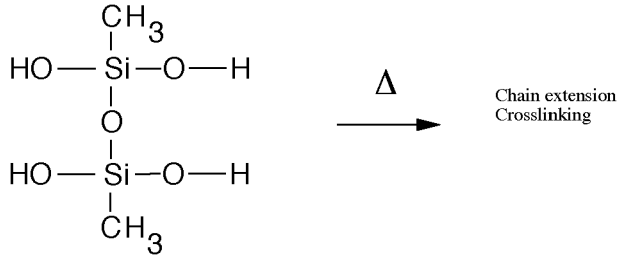

Scheme I Network formation from an idealized methylsilsesquioxane precursor.

‡Author to whom all correspondence should be addressed.

porosity and high pore contents can be produced economically by such methods, they are likely to be of interest not only as low ε insulating materials and in related applications such as low refractive index transparent coatings, but also as thermal insulating materials, where less stringent requirements may be placed on the matrix thermal stability than in electronics applications. There are nevertheless inherent processing problems associated with the plastification of polymer matrices by the degradation products and/or the need for degradation temperatures close to the matrix softening point (usually the glass transition temperature, T_g). This can lead to excessive deformation during the removal of the templates and hence to either collapse or blowing (expansion) of the pores, so that a heat resistant matrix is likely to remain necessary [11, 13]. Obtaining a suitable template morphology is also primordial to the design of such materials; usually one seeks a well-defined phase-separated microstructure with nanometric spherical inclusions of the labile phase up to high volume fractions of this latter. The correct length scales may be obtained using block copolymers with incompatible blocks, one of which constitutes the template, resulting in microphase separation with at least one characteristic length scale comparable to the block sizes. On the other hand, this does not necessarily lead to thermodynamically stable spherical morphologies at high incipient phase contents, depending on the relative chain stiffnesses and the molecular architecture [14].

An alternative is to use a template that is not initially chemically bonded to the matrix, but that is able to form the required phase separated morphology by controlled precipitation, induced by suitable drying or heat treatment of a cast film, or by chemical modification of one or both of the matrix and the template. Chemically induced phase separation (CIPS) is often exploited in the toughening of thermosets, entropic contributions to the free energy of an initially miscible mixture of the thermoset and the modifier decreasing as the crosslinking reaction proceeds and the matrix molar mass increases, leading eventually to precipitation [15]. If this occurs at a stage in the reaction where the overall molecular mobility is very low, a relatively fine dispersion of the incipient phase is usually observed, owing to suppression of the long-range transport processes responsible for growth and coalescence of the incipient phase domains. Indeed, if the gel point is reached before the mixture becomes thermodynamically unstable, the matrix may no longer be able to accommodate phase separation.

There has been particular interest in branched molecular architectures based on ε-polycaprolactone for templating PMSSQ. ε-polycaprolactone undergoes quantitative thermolysis at between 300 and 350°C, where appropriate prior heat treatments can render the matrix thermally stable, and PMSSQ has the advantage over SiO_2, say, of a relatively low ε (in the range 2.4 to 3.6). The templates are typified by dendrimers and hyperbranched polymers (HBPs) [16] and star-shaped [17] or star burst hyperbranched or dendrimer-like flexible chain polymers [18, 19]. The interest in dendritic polymers stems principally from the high density of chain ends, which facilitates compatibilisation with the matrix through suitable functional modification [20]. Nanoporous structures have been demonstrated in many cases, along with decreases in ε-consistent with a pore content corresponding to the initial template loading. Since the thermolysis of the PCL and its derivatives is clean, the excellent hydrophobicity of the PMSSQ is maintained, along with its hardness and thermal resistance up to 500°C, and $\varepsilon < 2$ is possible for void contents of 30 vol% or more, depending on the exact formulation of the matrix.

In the present work, rather than use molecular architectures based on relatively long flexible blocks synthesized *ad hoc*, we have investigated the extent to which porosity can be induced and controlled by simple end-functionalization of commercially available dendrimer-like hyperbranched aliphatic polyesters (HBP) [21] in order to compatibilize them with a MSSQ precursor. In a first approach, rather than functionalize with end-groups such as $Si(OEt)_3$, that are capable of reacting with the MSSQ [20], all or part of the ─OH groups of the as-received HBP have been converted to ─$OSiMe_3$, which is anticipated both to be compatible with the MSSQ (see the discussion) and to remain relatively inert during the initial stages of cure. It should therefore be possible to interpret solubility and hence morphological variations with the molar mass and degree of functionalization of the HBP, and the degree of MSSQ conversion qualitatively within a relatively simple thermodynamic framework, as in earlier work on CIPS in HBP blends with thermoset matrices [22–24].

2. Experimental

2.1. Starting materials and basic characterization

10 wt% MSSQ/BuOH (Filmtronics) was used throughout as the matrix precursor and appropriate processing conditions for PMSSQ network formation were chosen on the basis of dynamic mechanical analysis (DMA, Rheometrics RSA) of woven glass fiber ribbons coated with the precursor, following Nguyen *et al.* [17]. The results are shown in Fig. 1; after evaporation of the

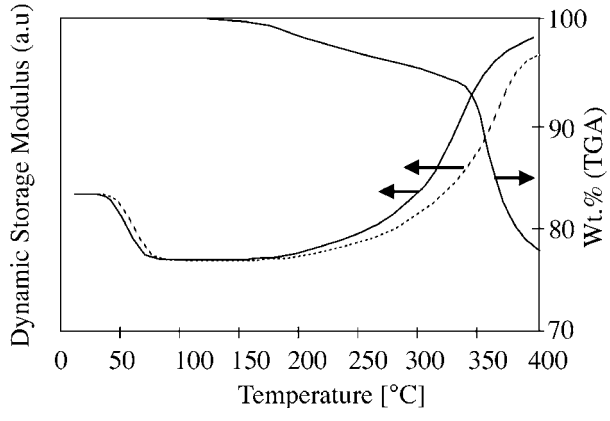

Figure 1 Dynamic storage modulus (1 Hz) as a function of temperature during ramping at 5 and 20 $Kmin^{-1}$ (dotted line) of a methylsilisesquioxane coated glass fibre braid along with weight loss measured by TGA as a funtion of temperature during ramping at 20 $Kmin^{-1}$.

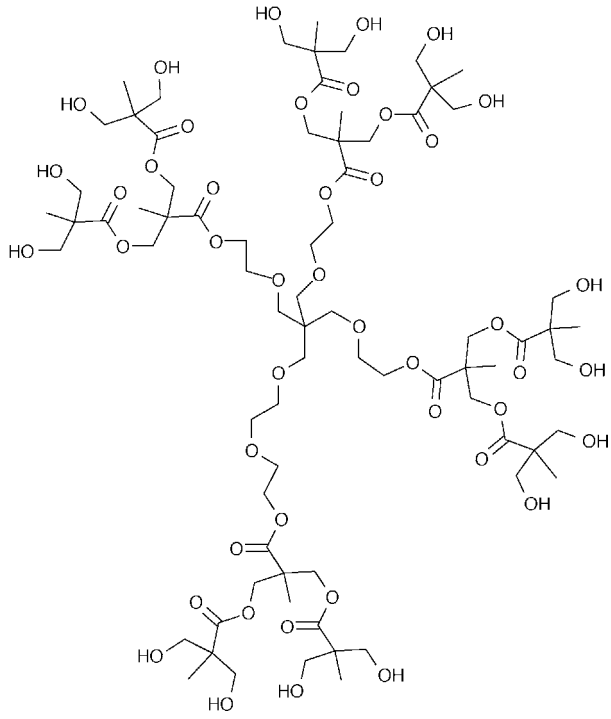

Scheme II Perfect 2 generation dendrimer analogue of the 2 pseudo-generation HBP.

solvent, the as-cast PMSSQ films were glassy at room temperature, softened above about 50°C and then began to chain-extend and crosslink at temperatures above about 200°C, depending on the scanning rate, becoming fully crosslinked above about 400°C.

Scheme II is an idealized representation of the aliphatic polyester HBP (Perstorp Chemicals). The structure shown is a homologous perfect 2 generation dendrimer with 16 ─OH functional groups per molecule. The corresponding HBP is prepared in a single "one pot" (or pseudo one pot) polycondensation of 2, 2 *bis*-hydroxymethyl propionic acid (*bis*-MPA) with a tetrafunctional ethoxylated pentaerythritol core. The different grades are designated by a pseudo-generation number by analogy with the perfect dendrimer, such that the n^{th} pseudo-generation corresponds to a reaction mixture containing

$$4\sum_{i=0}^{n-1} 2^i \qquad (1)$$

bis-MPA molecules for every core molecule. Nominal number average quantities can be derived assuming all the *bis*-MPA monomers to have reacted with a core molecule, so that the number average molar mass M_n, for example, is given by the total molar mass divided by the number of cores. Values calculated in this way are given in Table I, where they are denoted "dendrimer equivalent," Den_{eq}. Prior to use, the HBPs were reprecipitated to remove any oligomeric impurities. The HBP (30 g) was dissolved in methanol (200×10^{-6} m^3) at 50°C for 60 min and the warm methanol/HBP mixture slowly poured into vigorously stirred diethyl ether (400×10^{-6} m^3, 25°C) to give a fine white precipitate. The mixture was stirred for an additional 10 min and the polymer filtered off and dried under vacuum (267 Pa overnight at room temperature, then in a vacuum oven for 3 days at 80°C).

GPC measurements (Table I) were carried out on a Waters 150CV modified for on-line differential viscosimetry and universal calibration was used throughout [25]. ^{1}H-NMR spectra were recorded in $CDCl_3$ using a Bruker DPX-400 instrument with residual $CHCl_3$ ($\delta = 7.27$) as the internal reference. FTIR spectra were recorded in attenuated total reflection (ATR) mode using a Nicolet Magna DSP 650. Glass transition temperatures (Table I) were determined from differential scanning calorimetry (DSC, Perkin Elmer DSC7 calibrated with cyclohexane, water and indium) heating runs at 20 K min^{-1}. For hydroxy number determination (Table I) 0.5–0.6 g of dried HBP were weighed to the nearest 0.0001 g into a dry 250 ml flask, refluxed with 10.00×10^{-6} m^3 of 1:10 vol% acetic anhydride/dry pyridine at 115°C for 20–25 minutes and cooled to room temperature. Approximately 20×10^{-6} m^3 of acetone was added and the mixture titrated with 1.000 M NaOH using potentiometric monitoring (Metrohm Herisau Potentiograph E436).

2.2. Trimethylsilylation of HBPs: General procedure exemplified by a procedure for 100% trimethylsilylation of the 3 pseudo-generation HBP

A 250 ml three-necked round-bottomed flask was equipped with a reflux condenser, magnetic stir bar and oil bath, and purged three times with nitrogen. A portion of the 3 pseudo-generation HBP (1.81 g, 0.50 mmol) was weighed into the flask, followed by 50×10^{-6} m^3 dry tetrahydrofuran. The mixture was then heated to 65°C for 30–60 min, after which dissolution was substantially complete. Triethylamine (2.5×10^{-6} m^3, 1.8 g, 17.6 mmol) was added with a pipette, and chlorotrimethylsilane (2.0×10^{-6} m^3, 1.7 g, 16 mmol) added dropwise at 65°C, giving a white trimethylammonium hydrochloride precipitate. The reaction mixture was stirred for a further 30 min at 65°C and the heating bath then removed. After 10 min, the white precipitate was removed by filtration and the THF stripped off under vacuum. The remaining viscous oil was redissolved in 30×10^{-6} m^3 hexane and the residual insoluble ammonium salt removed by filtration. The hexane was stripped off in a rotary evaporator and drying completed under vacuum (39 Pa for 2 days). The product was a highly viscous liquid (1.95 g, 67%, ^{1}H-NMR (400 MHz, $CDCl_3$): δ4.27 (64H, ─COO─C$\underline{H}_2$─, broad s), 3.8–3.7 (92H, ─SiO─C$\underline{H}_2$─, HO─C$\underline{H}_2$─ and ─O─C$\underline{H}_2$─ (core), m), 1.3–1.0 (97H, ─C$\underline{H}_3$, m), 0.08 (277H, ─OSi─C$\underline{H}_3$, broad s).

2.3. Determination of the degree of trimethylsilylation

The degree of trimethylsilylation of the ─OH groups was calculated from ^{1}H-NMR (400 MHz, $CDCl_3$): The broad singlet at 4.3 ppm (Fig. 2), which is due to the ─COO─C$\underline{H}_2$─ protons, was set to 48 ppm (the 3 generation dendrimer equivalent value). Since the signal

TABLE I Physical data for the reprecipitated HBPs (M_n and M_w from GPC in dimethylformamide at 60°C). The T_g values are indicative, being very sensitive to the sample thermal history

	2 pseudo-generation	3 pseudo-generation	4 pseudo-generation
T_g [°C]	27	32	40
Den_{eq}—OH number [mmol —OH g^{-1}]	9.144	8.87	8.739
—OH number [mmol —OH g^{-1}]	8.69	8.25	8.03
$Den_{eq}M$[g mol^{-1}]	1750	3608	7323
M_n [g mol^{-1}]	2340	3510	3910
M_w [g mol^{-1}]	4560	7140	10060
Polydispersity (*PD*)	1.94	2.03	2.57

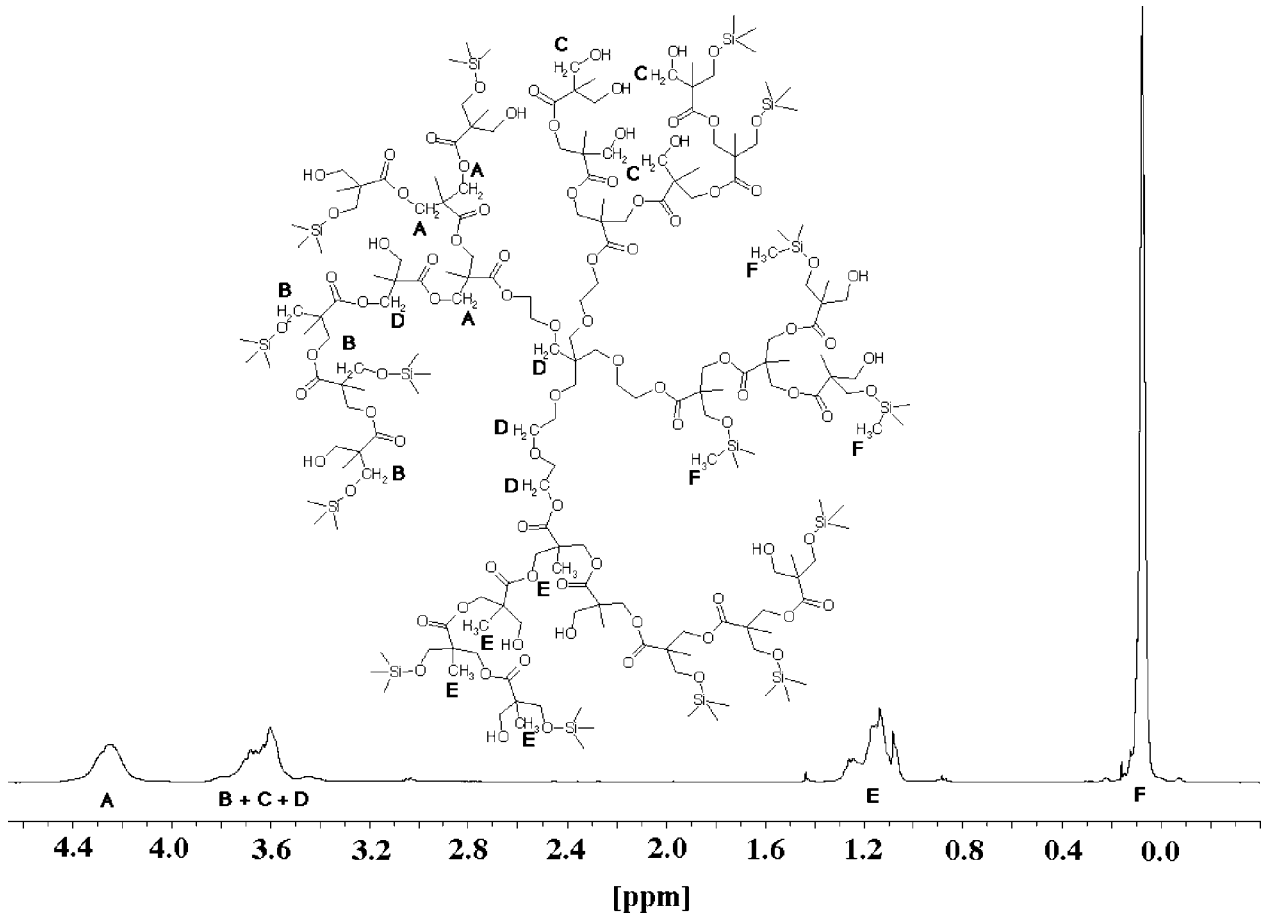

Figure 2 ^{1}H-NMR spectrum of a nominally 50% trimethylsiliylated 3 pseudo-generation HBP in $CDCl_3$. Proton positions associated with the chemical shifts are denoted by the corresponding letters on the spectrum and the drawing.

from the HO—C$\underline{H}_2$—/—SiO—C$\underline{H}_2$— protons (3.8–3.7 ppm) overlapped strongly with that associated with —O—C$\underline{H}_2$ protons from the core, the total number of the former was inferred from the —C$\underline{H}_3$ (1.3–1.0 ppm) and —COO—C$\underline{H}_2$— (4.27 ppm) signals. ^{1}H-NMR data for different stoichiometries and the corresponding estimated degrees of conversion are given in Tables II

TABLE II ^{1}H-NMR data and corresponding estimates of the degree of conversion from —OH to —$OSiMe_3$ for the 3 psuedo-generation HBP

	Nominal conversion of —OH to —$OSiMe_3$			
δ	25%	50%	75%	100%
4.27 ppm	48	48	48	48
3.8–3.7 ppm	68.3	76.5	66.75	69
1.3–1.0 ppm	74.3	72.75	73.5	72.75
0.08 ppm	48.8	105.75	159	207.75
Estimated conversion	21%	48%	71%	94%

for the III pseudo-generation HBP showing reasonable agreement with the nominal conversions inferred from the stoichiometry.

The GPC data in Table III for the 3 pseudo-generation HBP characterized using two different solvents were also consistent with the degrees of conversion calculated from ^{1}H-NMR. It was not thought to be possible to achieve full conversion by the present method, as also borne out by the IR spectra (Fig. 3). These showed a gradual decrease in the strength of the hydroxyl absorption band with increasing conversion, accompanied by an increase in the strength of the siloxane (C—O—Si) absorption peaks. Even with a four-fold excess of chlorotrimethylsilane and a reaction time of 4 hours (the HBP started to degrade after longer times), it was not possible to eliminate the —OH band, whose intensity stabilized at about 10% of its initial intensity as the amount of chlorotrimethylsilane was increased. The narrowing of both the —OH band and

TABLE III Physical data for the trimethylsilylated 3 psuedo-generation HBP (M_n and M_W from GPC in dimethylformamide and tetrahydrofuran)

	Nominal conversion of —OH to —$OSiMe_3$				
	0% Si	25% Si	50% Si	75% Si	100% Si
T_g [°C]	32	−17	−24	−30	−38
$Den_{eq}M$	3608	4184	4760	5336	5912
DMF M_n [g mol^{-1}]	3510	4280	5140	5560	6570
M_w [g mol^{-1}]	7140	8120	9350	9970	11800
PD	2.03	1.90	1.82	1.80	1.80
THF M_n [g mol^{-1}]	3510	4020	4980	5170	6120
M_w [g mol^{-1}]	6044	6880	8590	8850	10510
PD	1.72	1.71	1.72	1.71	1.72

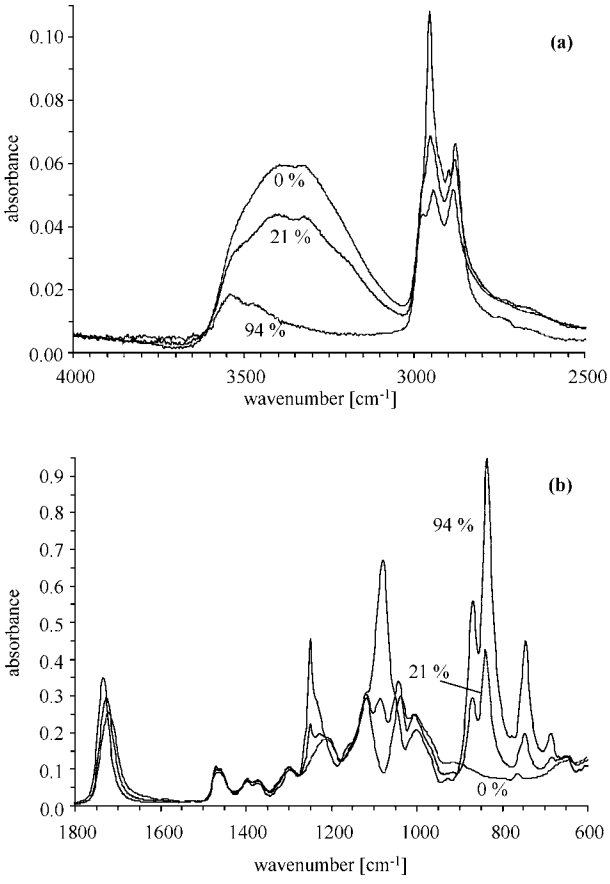

Figure 3 ATR-FTIR spectra of trimethylsilylated 3 pseudo-generation HBP with different degrees of trimethylsilylation; (a) O—H and C—H stretch region; (b) C═O and fingerprint region (absorption corrected for the wavelength dependence of the penetration depth and the band at 1300 cm^{-1} used for normalization).

the C═O stretch absorption peak, and the auxochromic shift of this latter indicated a decrease in H-bonding with increasing degree of trimethylsilylation. However the high wavenumber shoulder of the —OH band, near 2500 cm^{-1}, associated with absorption by uncoupled —OH groups showed little change, suggesting the residual unconverted —OH groups to be sterically hindered or shielded. Whatever their origin, these differences make it difficult to justify use of —OH band intensities to quantify the degree of conversion; the results from IR were nevertheless consistent with those from NMR.

2.4. Film preparation and morphological characterization

100 to 400 nm thick films were spin cast onto glass substrates at room temperature from the required amount of HBP immediately after mixing with the MSSQ precursor to a total of 10 wt% in BuOH. After air drying for one hour, the films were held at 90°C for 1 min, heated at 5 K min^{-1} to 425°C under dry N_2 and then held at 425°C for 30 min. For consistency, this heat treatment was maintained throughout, and no attempt was made to optimize the processing conditions further with respect to the final microstructures. Thermal gravimetric analysis data (Perkin Elmer TGA7, 2 K min^{-1}) are shown in Fig. 1 for a composite containing 20 wt% of the 100 % trimethylsilylated 3 pseudo-generation HBP, indicating quantitative degradation of the template starting at about 300°C. For transmission electron microscopy (TEM), the films were cast onto freshly cleaved KCl single crystals and recovered either before or after heat treatment by floating them onto carbon coated copper TEM grids (400 mesh) from distilled water and washing them twice in distilled water. The specimens were observed in bright field at 300 kV (Philips EM340) and pore volume fractions were estimated from the electron transmission of the films using a method described in detail elsewhere [26]. Pore diameters were estimated directly from the TEM images and the average values given in what follows are surface averages, that is, values weighted by the surface area of the pores. These provide a more realistic measure of the pore size than number averages, which tend to be very sensitive to the low pore diameter tail of the pore size distribution, which is in turn both difficult to characterize and accounts for a relatively small proportion of the overall porosity.

3. Results and discussion

A simple way of assessing the enthalpic contribution to the miscibility of organic species is to compare their solubility parameters, δ, estimated if necessary from the molecular structure. Here, δ has been calculated using van Krevelen and Fedors group contribution theory [27, 28]. Values for the different dendrimer equivalents and different degrees of conversion are listed in Table IV. The two methods gave consistent results, showing in each case a marked decrease in δ with increasing conversion of the —OH groups to —$OSiMe_3$. In calculating

TABLE IV Solubility parameters [$J^{1/2}$ $cm^{-3/2}$] estimated from group contribution methods (vK - Van Krevelen, F - Fedors) for trimethylsilylated dendrimers

		Nominal conversion of —OH to —$OSiMe_3$				
Generation	Method	0% Si	25% Si	50% Si	75% Si	100% Si
2	vK	26.2	22.9	20.6	18.8	17.3
	F	26.7	23.0	20.2	18.0	16.1
3	vK	26.2	23.0	20.7	18.9	17.4
	F	26.5	22.9	20.2	18.0	16.1
4	vK	26.1	23.0	20.8	19.1	17.5
	F	26.3	22.8	20.1	18.0	16.0

solubility parameter values for the MSSQ and PMSSQ it was necessary to make simplifying assumptions about the molecular architecture, namely the existence of a hypothetical monomer of the form $Si_2OMe_2(OH)_4$ from which ladder polymers such as shown in Scheme I are formed by condensation, giving a generic formula $(Si_2OMe_2)_nO_{2n-2}(OH)_4$. The corresponding van Krevelen and Fedors values for δ rapidly approach 16.5 and 14.5 $J^{1/2}$ $cm^{-3/2}$ respectively as n increases.

A first approximation to the Flory–Huggins interaction parameter, χ, for an HBP–solvent mixture is $s + (\delta_S - \delta_{HBP})^2 V_0/RT$, where V_0 is a reference volume that depends on the choice of lattice in the Flory–Huggins model for the free energy of mixing [29, 30], but is usually taken to correspond to the molar volume of the solvent molecules, and s is an empirical constant that accounts for non-enthalpic contributions to χ. Implicit here is that the interaction involves only dispersive forces. Although this may be justified in the present case for high degrees of trimethylsilylation, the presence of groups such as —OH may lead to non-negligible contributions to the overall solubility parameter from hydrogen bonding, which should strictly be considered separately when deriving χ using the solubility parameter approach [31]. Indeed in some lattice models for the solution behavior of dendritic polymers, the contribution from strong specific interactions to miscibility has been treated as a separate additive term to the free energy of mixing [32]. Any such approach is beyond the scope of the present work, however, for which the original Flory–Huggins lattice model [29, 30] is retained as a basis for simple qualitative discussion of the phase behavior of the MSSQ/HBP blends. The free energy of mixing, ΔG_m, in a monodisperse polymer–solvent system is then

$$\frac{\Delta G_m}{RT} = \frac{\phi}{x}\ln\phi + (1-\phi)\ln(1-\phi) + \chi\phi(1-\phi), \quad (2)$$

where ϕ is the polymer volume fraction and x is the number of lattice sites occupied by each polymer molecule. In the case of a polymerizable solvent, Equation 2 is replaced by

$$\frac{\Delta G_m}{RT} = \frac{\phi}{x}\ln\phi + \frac{(1-\phi)}{x_s}\ln(1-\phi) + \chi\phi(1-\phi) \quad (3)$$

where x_s is the degree of polymerization of the solvent (x and x_s are mass averages for a polydisperse system). This expresses at least qualitatively the dominant role of the enthalpic term for large x and x_s, leading to immiscibility for χ positive. If χ is independent of composition, the locus of the spinodal is given by the quadratic

$$\frac{1}{x\phi} + \frac{1}{x_s(1-\phi)} = 2\chi \approx \frac{2V_0(\delta_s - \delta_{HBP})^2}{RT} \quad (4)$$

Fig. 4 shows spinodals calculated from Equation 4 using the solubility parameters given in Table II for different degrees of trimethylsilylation and for different degrees of polymerisation of the MSSQ, for 2 and 4 generation dendrimer equivalents (binodal curves have been omitted for clarity, but show the same overall trends). Since the estimated solubility parameters varied relatively little with molar mass, the spinodals moved to higher temperatures with increasing molar mass for a given degree of trimethylsilylation. Thus, although trimethylsilylation was inferred to improve the solubility of both 2 and 4 pseudo-generation HBPs in the MSSQ precursor, the 4 pseudo-generation HBP was anticipated to be far less soluble than the 2 pseudo-generation trimethylsilylated HBP, particularly at low HBP concentrations. Although quantitative interpretation is more difficult, given the severe limitations of models of this type, it is noteworthy that at intermediate compositions, the 4 generation 100% trimethylsilylated dendrimer was predicted to become insoluble at relatively low degrees of polymerisation of the MSSQ in the vicinity of 200°C, where significant cure took place in the real system (Fig. 1). On the other hand, the 2 generation 100% trimethylsilylated dendrimer equivalent was predicted to remain soluble under these conditions. This implies phase separation at a much earlier stage in the heat treatment for the higher molar mass HBP

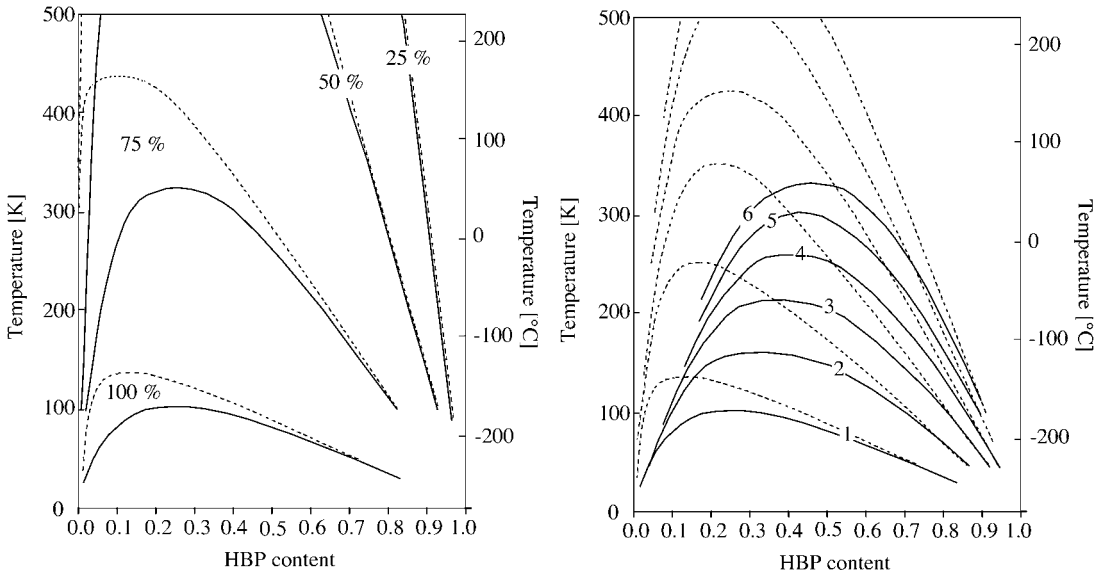

Figure 4 Estimated spinodals for 2 generation (solid curves) and 4 generation dendrimers (hatched curves) for (a) different degrees of trimethylsilylation in a monomeric precursor matrix and (b) for different degrees of matrix polymerization and 100% trimethylsilylation.

and, based on simple kinetic arguments invoked previously to describe CIPS in functionalised HBP/epoxy resin blends [23], a coarser final microstructure. It follows from Fig. 4 that the scale of the final microstructure should also be composition dependent, with coarser microstructures being expected for higher HBP contents. Moreover, for HBP contents beyond the composition corresponding to the critical point, which corresponds very roughly to the maximum of the spinodal, the incipient phase is expected to be matrix-rich. Thus, the sought after morphology of discrete HBP-rich domains in a continuous PMSSQ matrix up to high HBP contents was thought most likely to be acheivable by using the low molar mass 2 pseudo-generation HBP, for which the phase diagram was predicted to become approximately symmetric at relatively low degrees of MSSQ polymerisation.

Fig. 5 provides an indication of the miscibility of various HBPs with the MSSQ precursor, based on observations of films spin cast from BuOH at different temperatures. Also included in the figure are results for ─OH terminated polycaprolactone (PCL) star polymers derived from 3 pseudo-generation HBP cores, with arm lengths of 10 to 30 monomer units, synthesized following a literature procedure [33]. It should be stressed that the results in Fig. 5 cannot be considered to represent equilibrium conditions because of the nature of the film casting process and the presence of the solvent. In all cases, homogenous solutions in BuOH and optically transparent cast films could be obtained, but the ─OH terminated HBPs and PCL stars generally required dissolution and casting temperatures of the order of 60°C or more. Films cast in this temperature range showed poor wetting on glass substrates and tended to crack more readily in the presence of the modifiers than films cast at room temperature. The microstructures shown in Fig. 6 and Fig. 7a were obtained by drying at the dissolution/casting temperature and heating directly to 90°C, i.e. the first stage of the heat treatment. The scale of the porosity was difficult to control at higher loadings, processing leading to coarse, partially collapsed structures, and cloudy or opaque films. Relatively fine pores were obtained in films containing 5 wt% HBP-g-CL_{10} cast at 60°C as shown in Fig. 6b, but the pore diameters were highly polydisperse.

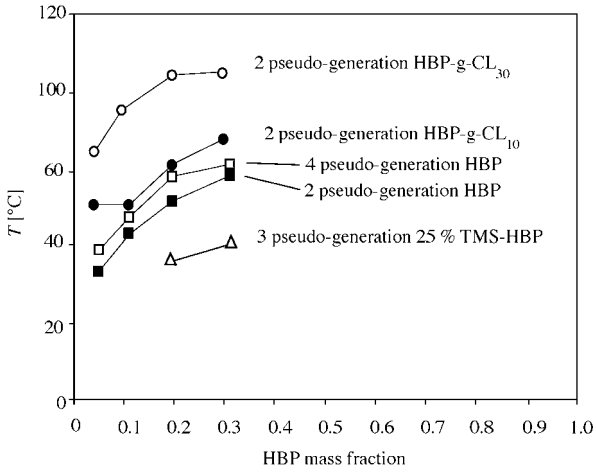

Figure 5 Pseudo-cloud point curves for various HBPs and modified HBPs in MSSQ as determined from optical microscopy and TEM of films cast from BuOH solution (10 wt% solids content) and stained with RuO_4 (the films were heterogeneous in the region below the curves in each case).

The results for the nominally 25% trimethylsilylated 3 pseudo-generation HBP given in Fig. 5 were consistent with the predicted improvement in compatibility between the HBP and the MSSQ with increasing levels of trimethylsilylation, with higher degrees of trimethylsilylation leading to homogeneous as-cast films at room temperature over a wide range of compositions. As shown in Fig. 7, the improved compatibility on trimethylsilylation was also reflected by a decrease in the maximum pore diameter in the heat-treated films. Moreover, in qualitative agreement with the predicted behavior, there was a systematic decrease in pore size with decreasing pseudo-generation number at fixed composition, illustrated in Fig. 8 for films containing 30 wt% 100% trimethylsilylated HBPs.

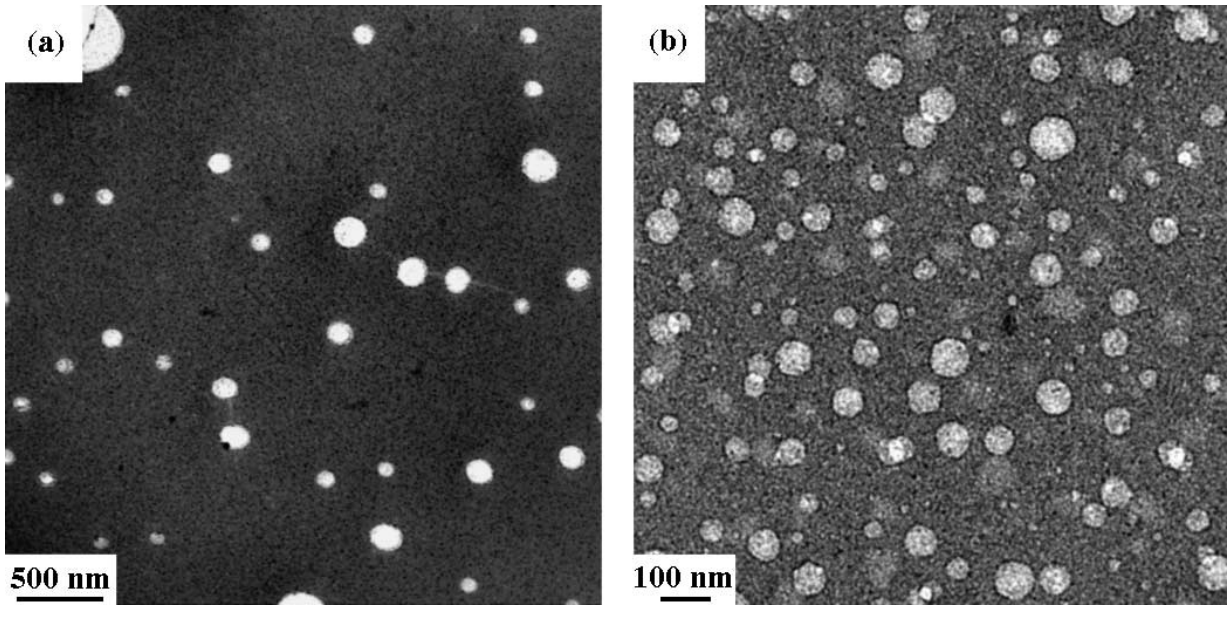

Figure 6 TEM of porous silicates prepared from MSSQ blends with (a) 15 wt% HBP-g-CL_{10} and (b) 5 wt% HBP-g-CL_{10} cast at 60°C.

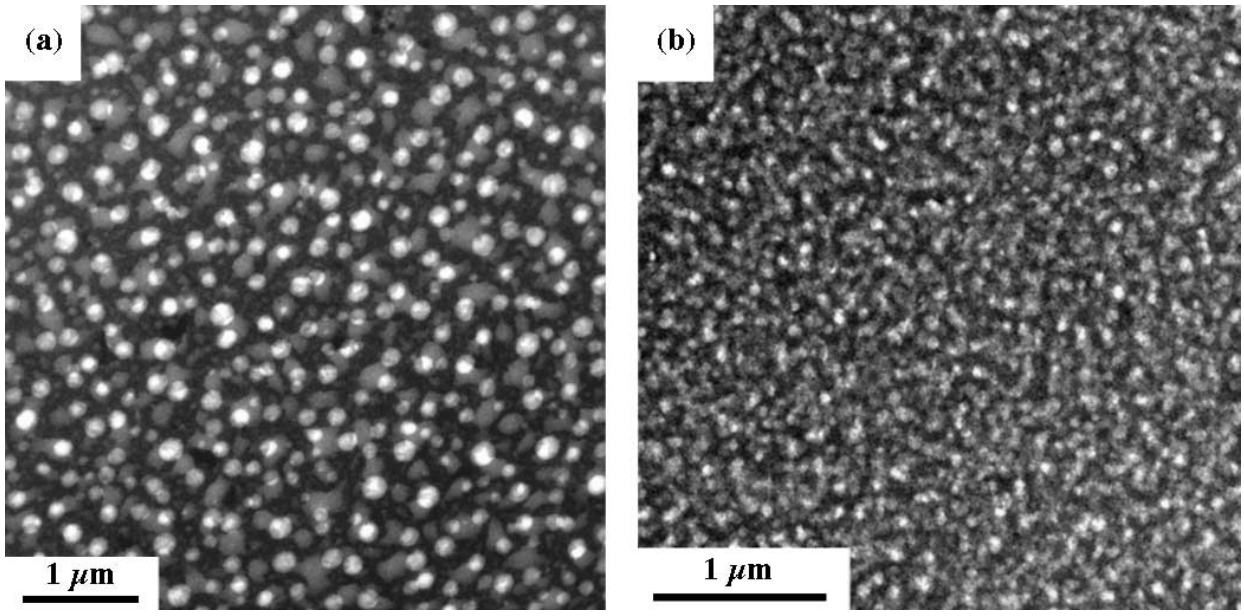

Figure 7 TEM of porous silicates prepared from MSSQ blends with (a) 20 wt% 4 pseudo-generation HBP and (b) 20 wt% 100% trimethylsilylated 4 pseudo-generation HBP cast at 60°C and room temperature respectively.

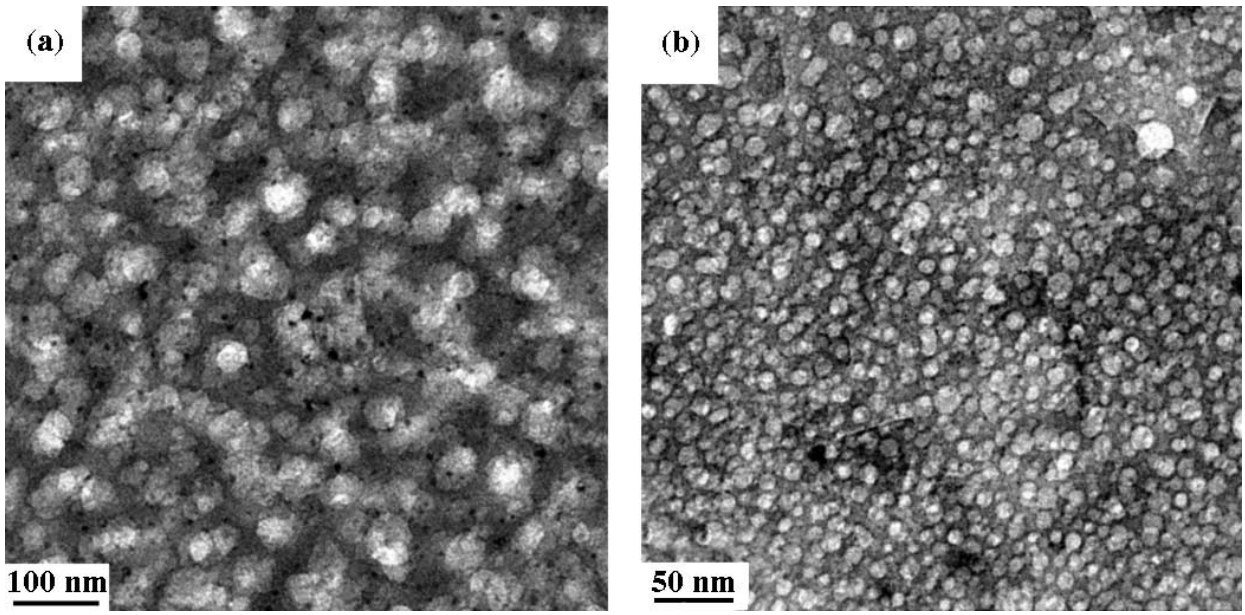

Figure 8 TEM of porous silicates prepared from MSSQ blends with (a) 30 wt% 100% trimethylsilylated 4 pseudo-generation HBP and (b) 30 wt% 100% trimethylsilylated 2 pseudo-generation HBP cast at room temperature.

Atomic force microscopy (AFM) (Park Instruments, Autoprobe CP) provided a convenient alternative method for rapid assessment of the trends in the film microstructures as a function of the additive type, and although limited to measures of the surface morphology and somewhat harder to interpret rigorously, the results correlated well with those from TEM. Moreover they suggested that the final microstructure did not vary significantly with film thickness in films that were homogeneous as-cast. The example in Fig. 9 shows intermittent contact mode AFM height images of heat treated, approximately 400 nm thick MSSQ/3 pseudo-generation HBP film with different degrees of trimethylsilylation of the HBP, illustrating the trend towards finer pore sizes with increased trimethylsilylation.

The quantitative TEM observations are summarized in Fig. 10. Good control of pore sizes was achieved over a relatively wide range of compositions and the final porosity increased steadily with the modifier weight fraction. The films were transparent up to the highest film thicknesses investigated in the range of compositions shown. However at and close to 50 wt% HBP, the films phase separated on heat treatment to give a co-continuous morphology, which in turn led to widespread cracking during processing, and opaque films. In general, the final microstructures contained pores with dimensions much greater than those that would be associated with single HBP molecules, the external diameters of the dendrimer analogues being in the 2 to 3 nm range as determined by self-avoiding rotational isomeric state simulations

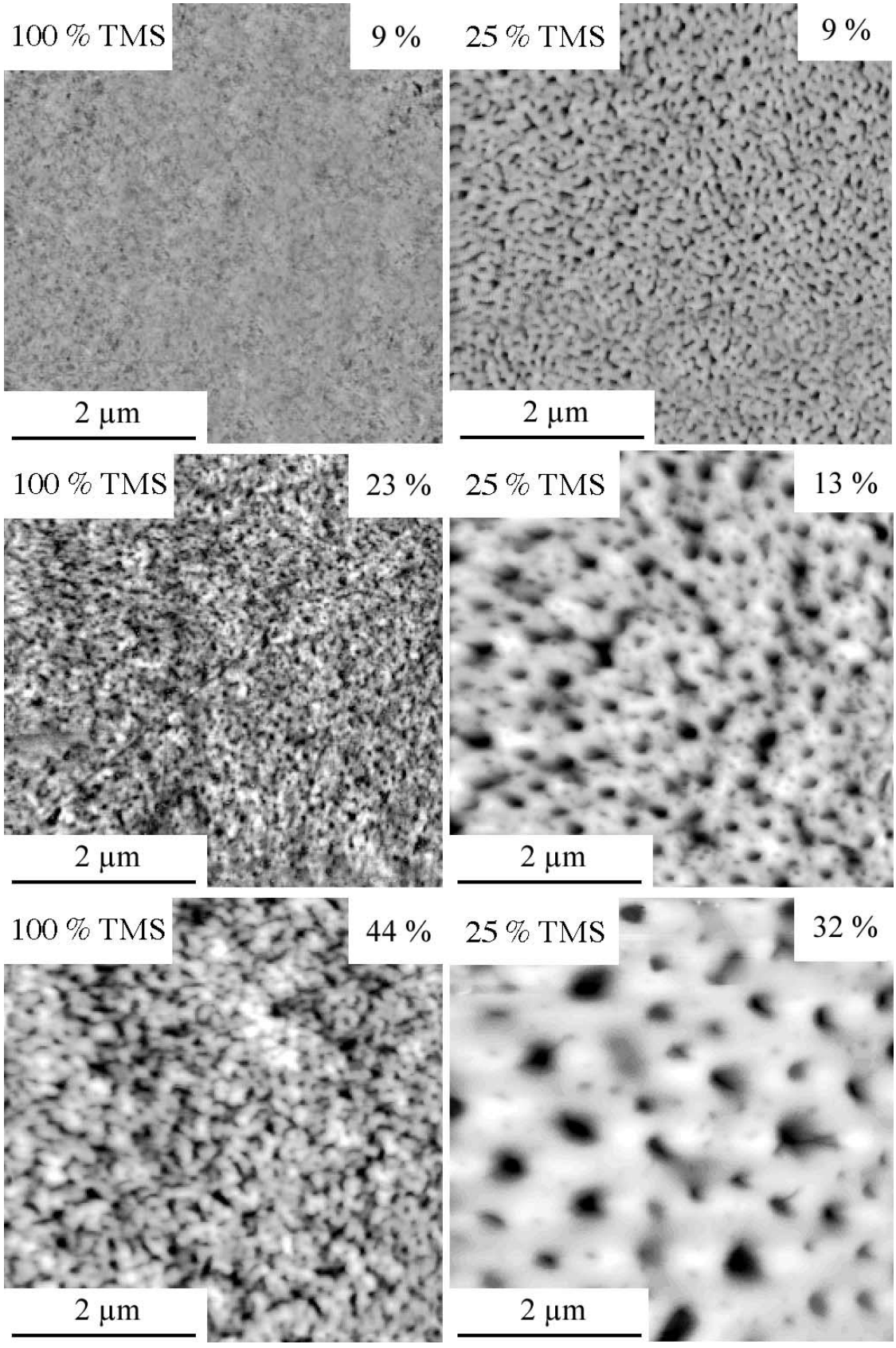

Figure 9 AFM images (of heat treated 400 nm thick MSSQ/3 pseudo-generation HBP films with 25 and 100% trimethylsilylation (intermittent contact mode height images).

of isolated molecules. Thus even the smallest observed average pore sizes would correspond to about 100 such molecules, so that their size does not directly control the microstructure as it would in the case of single molecule micelles, say. Moreover, the kinetic aspects of the phase separation do not appear to be strongly influenced by the size of the HBP in so far as the trend is towards coarser microstructures with increasing HBP pseudo-generation number; one would expect any decrease in molecular mobility associated with the increasing generation number to lead to finer microstructures (for a given matrix mobility).

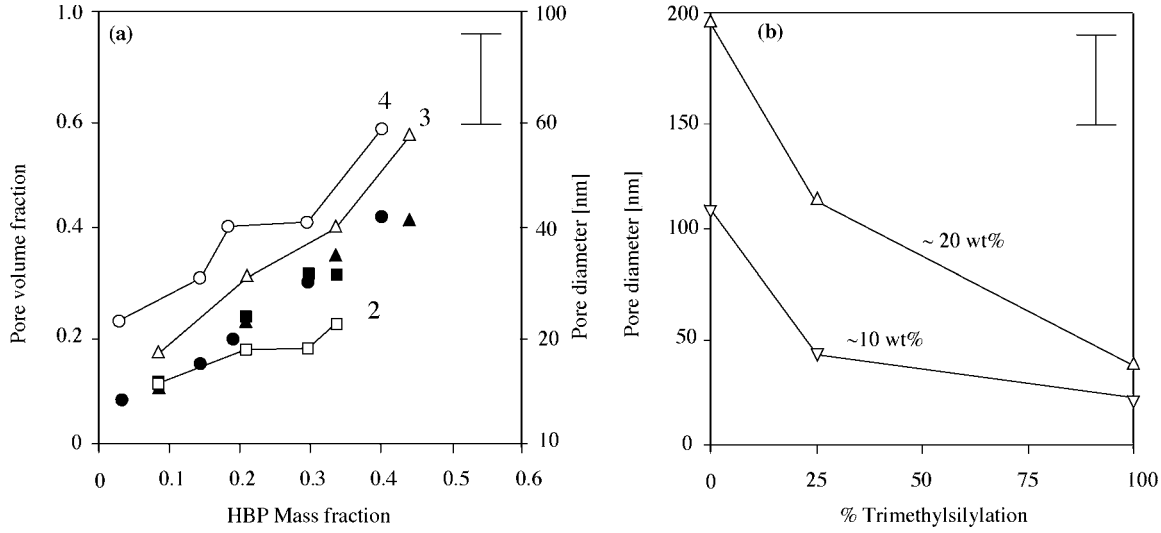

Figure 10 (a) Average pore diameters (open symbols) and pore volume fractions (filled symbols) in heat treated blends of MSSQ with 100% trimethylsilylated 2 to 4 pseudo-generation HBPs as indicated; (b) Average pore diameters in 3 pseudo-generation HBPs for different degrees of trimethylsilylation for the approximate compositions indicated.

4. Conclusion

Nanoporous films have successfully been prepared using trimethylsilylated HBPs in MSSQ and standard heat treatment conditions. The avoidance of expensive *ad hoc* reagents, and the simple chemistry and fabrication offer promise and there is still considerable scope for further optimizing the pore sizes and increasing the pore volume fractions, both through optimization of the process conditions and by varying the end-group chemistry. For example, $-OSi(OEt)_3$ end-groups would react with the silicate precursor and $-O(CH_2)_3SiMe_3$ is anticipated to be more stable than $-OSiMe_3$ with respect to long term storage in BuOH and to alcoholysis during film preparation. $-OSiMe_3$ nevertheless provides a convenient model for the study of chemically induced phase separation in methylsilsesquioxanes and there remains a substantial body of characterization that should be undertaken in order provide a more detailed understanding of the results presented here. In particular it will be necessary to investigate the curing kinetics and molecular weight build-up in the methylsilsesquioxane during the heat treatment, and carry out *in situ* investigations of the phase separation process during cure in order to determine its dependence on the degree of conversion of the matrix. At the same time, it is intended to extend the work to template other organic–inorganic and organic systems using the same basic approach.

Acknowledgments

The authors are grateful for the financial support of the Swiss CTI Top Nano 21 initiative and for the technical support of the Centre Interdépartemental de Microscopie Electronique (CIME) of the EPFL.

References

1. G. MAIER, *Prog. Poly. Sci.* **26** (2001) 3.
2. M. T. BOHR, *Solid State Technol.* **9** (1996) 105.
3. J. C. MAXWELL-GARNETT, *Philos. Trans. R. Soc. Lon.* **205** (1905) 237.
4. D. J. BRINKER and G. W. SCHERRER, "Sol-Gel Science: The Physics and Chemistry of Sol-Gel Processing" New York, Academic, 1990.
5. Y. LU, R. GANGULI, C. A. DREWIEN, M. T. ANDERSON, C. J. BRINKER, W. GONG, Y. GUO, H. SOYEZ, B. DUNN, M. H. HUANG and J. I. ZINK, *Nature* **389** (1997) 364.
6. J. L. HEDRICK, J. W. LABADIE, T. P. RUSSELL, D. HOFER and V. WAKHARHAR, *Polymer* **34** (1993) 4717.
7. J. L. HEDRICK, T. P. RUSSELL, J. LABADIE, M. LUCAS and S. SWANSON, *ibid.* **36** (1995) 2685.
8. J. L. HEDRICK, C. J. HAWKER, R. DIPIETRO, R. JERÔME and Y. CHARLIER, *ibid.* **36** (1995) 4855.
9. Y. CHARLIER, J. L. HEDRICK, T. P. RUSSELL, A. JONES and W. VOLKSEN, *ibid.* **36** (1995) 987.
10. J. L. HEDRICK, R. DIPIETRO, C. J. G. PLUMMER, J. G. HILBORN and R. JERÔME, *ibid.* **37** (1996) 5229.
11. J. L. HEDRICK, K. R. CARTER, J. W. LABADIE, R. D. MILLER, W. VOLKSEN, C. J. HAWKER, D. Y. YOON, T. P. RUSSELL, J. E. MCGRATH and R. M. BRIBER, *Adv. Polym. Sci.* **141** (1998) 1.
12. J. F. REMENAR, C. J. HAWKER, J. L. HEDRICK, S. M. KIM, R. D. MILLER, C. NGUYEN, M. TROLLSÅS and D. Y. YOON, *Mater. Res. Soc. Symp. Proc.* **511** (1998) 69.
13. J. L. HEDRICK, J. W. LABADIE, W. VOLKSEN and J. G. HILBORN, *Adv. Poly. Sci.* **147** (1999) 61.
14. I. W. HAMLEY, "The Physics of Block Copolymers" (Oxford University Press, Oxford, 1998).
15. R. J. J. WILLIAMS, B. A. ROZENBERG and J.-P. PASCAULT, *Adv. Poly. Sci.* **128** (1997) 95.
16. C. NGUYEN, C. J. HAWKER, R. D. MILLER, E. HUANG, J. L. HEDRICK, R. GAUDERON and J. G. HILBORN, *Macromolecules* **33** (2000) 4281.
17. C. V. NGUYEN, K. R. CARTER, C. J. HAWKER, J. L. HEDRICK, R. L. JAFFE, R. D. MILLER, J. F. REMENAR, H.-W. RHEE, P. M. RICE, M. F. TONEY, M. TROLLSÅS and D. Y. YOON, *Chem. Mat.* **11** (1999) 3080.
18. J. L. HEDRICK, M. TROLLSÅS, C. J. HAWKER, B. ATTHOF, H. CLAESSON, A. HEISE, R. D. MILLER, D. MECERREYES, R. JÉRÔME and P. DUBOIS, *Macromolecules* **31** (1998) 8691.
19. D. MECERREYES, E. HUANG, T. MAGBITANG, W. VOLKSEN, C. J. HAWKER, V. Y. LEE, R. D. MILLER and J. L. HEDRICK, *High Performance Polymers* **13** (2001) s11.
20. J. L. HEDRICK, C. J. HAWKER, R. D. MILLER, R. TWEIG, S. A. SRINIVASAN and M. TROLLSÅS, *Macromolecules* **30** (1997) 7607.
21. E. MALMSTRÖM, M. JOHANSSON and A. HULT, *ibid.* **28** (1995) 1698.

22. L. BOOGH, B. PETTERSSON and J.-A. E. MANSON, *Polymer* **40** (1999) 2249.
23. R. MEZZENGA, C. J. G. PLUMMER, L. BOOGH and J.-A. E. MÅNSON, *ibid.* **42** (2001) 305.
24. C. J. G. PLUMMER, R. MEZZENGA, L. BOOGH and J. A. E. MÅNSON, *Polym. Eng. Sci.* **41** (2001) 43.
25. L. GARAMSZEGI, T. Q. NGUYEN, C. J. G. PLUMMER and J.-A. E. MÅNSON, to appear in Macromolecular Physics and Chemistry.
26. C. J. G. PLUMMER, J. L. HEDRICK and J. G. HILBORN, *Polymer* **36** (1995) 2485 .
27. D. W. VAN KREVELEN, "Properties of Polymers" 3rd ed. (Elsevier, Amsterdam, 1990).
28. R. F. FEDORS, *Polym. Eng. Sci.* **14** (1974) 147.
29. P. J. FLORY, *J. Chem. Phys.* **10** (1942) 51.
30. M. L. HUGGINS, *Ann. N.Y. Acad. Sci.* **42** (1942) 1.
31. C. M. HANSEN, *J. Paint Technology* **39** (1967) 505.
32. J. G. JANG and Y. C. BAE, *J. Chem. Phys.* **114** (2001) 5034.
33. M. TROLLSÅS, J. L. HEDRICK, D. MECERREYES, P. DUBOIS, R. JÉRÔME, H. IHRE and A. HULT, *Macromolecules* **30** (1997) 8508.

Received 11 February
and accepted 10 May 2002